Published in final edited form as:
Bone. 2009 July ; 45(1): 52–60. doi:10.1016/j.bone.2009.03.675.

Rho GTPase Signaling and PTH 3–34, but not PTH 1–34, Maintain the Actin Cytoskeleton and Antagonize Bisphosphonate Effects in Mouse Osteoblastic MC3T3-E1 Cells

Nikolas H. Kazmers, **Sophia A. Ma**, **Tomohiko Yoshida**, and **Paula H. Stern**
Department of Molecular Pharmacology and Biological Chemistry, Northwestern University Feinberg School of Medicine, Chicago, IL 60611

Abstract

Cytoskeletal elements are critical for cell morphology and signal transduction, and are involved in many cellular processes including motility, intracellular transport, and differentiation. Small GTP-binding proteins (G proteins) of the Ras family, such as RhoA, influence various elements of the cytoskeleton. RhoA stabilizes the actin cytoskeleton and promotes formation of focal adhesions. We found previously that RhoA is expressed in osteoblastic cells and is translocated to the plasma membrane and activated by PTH 1–34 as well as by Nleu^{8,18} Tyr^{34} PTH 3–34 amide, a PTH analog that does not increase cAMP. We therefore investigated effects of manipulating RhoA on the actin cytoskeleton of osteoblastic MC3T3-E1 cells. Three inhibitors were used: 1) GGTI-2166, a geranylgeranyl transferase I inhibitor that prevents the isoprenylation and membrane translocation of RhoA, 2) Y-27632, a Rho kinase inhibitor, and 3) alendronate, a nitrogen (N)-containing bisphosphonate that reduces intracellular geranylgeranylpyrophosphate through inhibiting farnesyl pyrophosphate synthase. To increase RhoA activity, we used the geranylgeranyl group donor geranylgeraniol (GGOH), and a constitutively active RhoA. The F-actin cytoskeleton and focal adhesions (FA) were visualized with rhodamine-phalloidin and fluorescent anti-vinculin antibodies, respectively. Cells were imaged with confocal microscopy. Actin stress fiber density, edge actin bundle density, focal adhesion density, cellular area and circularity (a morphological descriptor relating area and perimeter) were quantified by a program developed with Matlab® software. GGTI-2166, Y-27632, and alendronate reduced actin stress fibers, FA density, and FA size, but had no effect on edge actin bundle density, cellular area, or circularity. GGOH completely antagonized the effects of alendronate, but did not significantly affect responses to GGTI-2166 or Y-27632. Constitutively active RhoA antagonized the effects of alendronate and GGTI-2166, but not those of Y-27632. The effects of alendronate were also antagonized by Nleu^{8,18} Tyr^{34} PTH 3–34 amide, but not by PTH 1–34. The results indicate that RhoA is involved in the maintenance of stress fibers and focal adhesions in osteoblastic cells, that PTH can affect this pathway independently of cAMP, and that a N-containing bisphosphonate can affect the actin cytoskeleton and focal adhesions through actions on geranylgeranyl groups and potentially through RhoA. In view of the importance of the actin cytoskeleton, the findings constitute evidence that N-containing bisphosphonates, when they attain certain concentrations, have effects on osteoblasts that could influence bone remodeling.

Corresponding author: Dr. Paula Stern, Department of Molecular Pharmacology and Biological Chemistry, Northwestern University Feinberg School of Medicine, 303 E. Chicago Ave. S-215, Chicago, IL 60611, Phone: (312) 503-8290, FAX: (312) 03-5349, Email: p-stern@northwestern.edu.

Keywords

osteoblast; cytoskeleton; RhoA; bisphosphonate; parathyroid hormone

INTRODUCTION

The actin cytoskeleton is integral to many cellular processes including survival, migration, proliferation, differentiation, and cell-cell communication [1]. Since the dysregulation of these processes in osteoblasts could contribute to diseases such as osteoporosis by interfering with the normal maintenance of bone architecture and metabolism, it is important to understand the signaling pathways and intermediates that modulate the osteoblast actin cytoskeleton. It is known that the small G protein RhoA, when active in its geranylgeranylated and GTP-bound form, is capable of maintaining the actin cytoskeleton [2]. Since N-containing bisphosphonates such as alendronate inhibit farnesyl pyrophosphate synthetase [3], an enzyme in the mevalonate pathway needed to produce geranylgeranyl groups, they could affect the actin cytoskeleton through impairing the activation of RhoA. Parathyroid hormone (PTH) 1–34 and $Nleu^{8,18}$ Tyr^{34} PTH 3–34 amide (PTH 3–34) activate RhoA in osteoblastic cells [4], suggesting that parathyroid hormone could act to stabilize the osteoblast actin cytoskeleton. Since PTH 1–34 inhibits actin polymerization and promotes the disassembly of components of the actin cytoskeleton [5–8] through cAMP-dependent mechanisms [5,6], its effects on the actin cytoskeleton are likely to be more complex than those of PTH 3–34, which has limited or no stimulatory effects on cAMP [9,10].

The experiments herein investigated the effects of RhoA, and factors affecting its activation and action, on the integrity of actin stress fibers, edge actin bundle, and focal adhesions in MC3T3-El cells as well as on the shape and area of the cells. Changes in the cytoskeletal structures were quantified after treatment of the cells with inhibitors: the geranylgeranyltransferase I inhibitor GGTI-2166 [11], the Rho kinase inhibitor Y-27632 [12], and the N-containing bisphosphonate alendronate, and stimulators: a constitutively active RhoA construct and geranylgeraniol (GGOH), an exogenous source of geranylgeranyl groups. A model for the observed interactions based on the experimental results provides a mechanism by which bisphosphonates could affect osteoblasts in addition to their well-established actions on osteoclasts. In addition, PTH 3–34, but not PTH 1–34, antagonized the alendronate-induced reduction in actin stress fibers.

MATERIALS & METHODS

Materials

GGTI-2166 was provided by Dr. Said Sebti, Moffitt Cancer Center and Dr Andrew Hamilton, Yale University. The constitutively active RhoA was provided by Dr Sebti. Y-27632 was purchased from Calbiochem. Geranylgeraniol was purchased from BioMol. Bovine PTH 1–34 and $Nleu^{8,18}Tyr^{34}$ bPTH 3–34 amide were purchased from BaChem. Alendronate was a generous gift from Alfred Reszka, Merck Research Laboratories.

Cell Culture

MC3T3-E1 subclone 4 pre-osteoblast cells were maintained in α-MEM supplemented with 10% fetal bovine serum (FBS) and 1% penicillin-streptomycin (PS) (FBS medium) at 37°C in a humidified atmosphere of 5% CO_2 in air. Media were replaced every three days, and the cells were subcultured weekly for use in experiments within six passages of the initial plating. For experiments, cells were seeded on 22 mm^2 glass coverslips coated with rat type I collagen which had been placed into six-well plates. A seeding density of 40,000 cells/well was used

in transfection experiments, and 25,000 cells/well was used in all other experiments. Cells were allowed to adhere and grow for 24 hours before treatments were started. Treatments were for either 6 hr or 22 hr, as indicated in the Results and Figure Legends, α-MEM supplemented with 0.1% bovine serum albumin (BSA) and 1% PS (BSA medium) was used for 6 hr treatments. FBS medium was used for 22 hr treatments.

Transient Transfection

MC3T3-E1 cells seeded on type I collagen-coated coverslips at a density of 40,000 cells/well were transiently transfected as previously described [4]. For each coverslip, 1 μg of the appropriate DNA construct (the constitutively active RhoA construct RhoA63L, or pcDNA as a control) and 2 μl PLUS reagent (Invitrogen) were first brought to a volume of 100 μl in OPTI-MEM. Following incubation of the DNA and PLUS reagent for 15 minutes at room temperature, 3 μl Lipofectamine (Invitrogen) and 97 μl OPTI-MEM were added to the mixture, which was then incubated at room temperature for 15 minutes. Each coverslip was treated with 200 μl of the resulting DNA mixture combined with 800 μl OPTI-MEM for three hours in a tissue culture incubator. Each coverslip then received 1 ml OPTI-MEM supplemented with 5% FBS and 100 U/ml penicillin, and was incubated for an additional 15 hours in the tissue culture incubator. At this point, treatment of the cells with GGTI-2166, Y-27632, or alendronate was initiated as appropriate. A pcDNA empty vector control was used in all transfection experiments.

Labeling of the F-Actin Cytoskeleton and Focal Adhesions for Confocal Microscopy

MC3T3-E1 cells grown on collagen-coated coverslips were fixed with 2.0% paraformaldehyde in PBS and permeabilized with 0.1% Triton X-100 in PBS. Blocking solution (1.2% BSA in PBS) was used to block non-specific antibody binding. To label focal adhesions, cells were treated with mouse anti-vinculin primary antibody (1:50 dilution in blocking solution) for 35 minutes followed by a 35 minute treatment with FITC-conjugated goat anti-mouse antibody (1:100 dilution in blocking solution). Rhodamine-phalloidin (1:40 dilution in blocking solution) was then added to label the F-actin cytoskeleton. Coverslips were mounted on glass microscope slides using an anti-fade mounting medium and sealed with clear nail polish. Cells were viewed on an Olympus Fluoview 1×70 confocal scanning laser microscope using a 60x oil-immersion lens, and digital images were captured in TIFF format using Olympus Fluoview software. Only cells not in contact with other cells were imaged.

Image Quantification

An image quantification program was developed in Matlab® to assess each cell image for its actin stress fiber density, edge actin bundle density, focal adhesion density and average size, and cellular area and circularity. For each cell under examination, the input into the program included three separate images extracted from the original confocal micrograph, including an image of the F-actin + vinculin overlap (Figure 1A), F-actin alone (Figure 1B), and vinculin alone (Figure 1C). The F-actin + vinculin image was converted to binary, and the cellular area and perimeter were calculated. As a metric of cellular morphology, cellular circularity was calculated (circularity = $4\pi(\text{area})/\text{perimeter}^2$; a circularity of 1.0 indicates perfect circular morphology, and 0.0 indicates a line). The perimeter of the cell was dilated to a width of 2.5 μm (Figure 1D) in order to define the internal (gray) and perimeter (blue) regions of the cell, which correspond with the locations of the actin stress fibers and actin edge bundle, respectively. The F-actin image (Figure 1B) was normalized for average pixel intensity, intensity-thresholded to minimize background fluorescence, converted to binary, and extraneous objects with an area of $\leq 0.5\ \mu m^2$ were removed. The resulting image was subjected to a Canny filter edge-detecting algorithm, producing an image (Figure 1E) depicting the edges of F-actin fibers in the perimeter (green – edge actin bundle) and internal regions of the cell

(red – stress fibers). This image was thresholded by aspect ratio of each detected edge to remove circular non-filamentous artifacts. The area occupied by F-actin edge was computed separately in both the perimeter and internal regions of the cell. The stress fiber density and edge actin bundle density were calculated by normalizing the area occupied by F-actin edge in the internal and perimeter regions of the cell (Figure 1E) by the area of the internal and perimeter regions (Figure 1D), respectively. To quantify the focal adhesion density and average size, the vinculin image (Figure 1C) was intensity-thresholded to reduce background fluorescence, converted to binary, and extraneous objects $\leq 0.3\ \mu m^2$ [13] were removed (Figure 1F). Focal adhesion density (focal adhesions per cellular area) and average focal adhesion size were calculated for the cell as a whole. Figure 1G depicts the focal adhesions that were detected based on these criteria (red = internal focal adhesion; green = perimeter focal adhesion; yellow arrow = vinculin aggregate below area threshold of $0.3\ \mu m^2$). For experiments in which actin was studied alone, the vinculin quantification functionality was disabled.

Statistical Analysis

Statistical significance was determined based on 95% Tukey confidence intervals of the differences between groups that were obtained from one-way ANOVA ($\alpha=0.05$). Residuals from ANOVA were analyzed for normality and constant inter-group variance, and when necessary, Box-Cox transformation was conducted on data displaying non-constant inter-group variance. A 95% confidence level ($\alpha=0.05$) was used as the threshold for statistical significance. Minitab® software (Version 14) was used for all statistical analyses.

RESULTS

The initial experiments were designed to determine whether Rho A was important for the actin cytoskeleton of MC3T3-E1 cells. For these studies, two inhibitors were used. The geranylgeranyl transferase I inhibitor GGTI-2166 was used to prevent the geranylgeranylation step, considered to be critical for membrane translocation and subsequent activation of Rho small G proteins, including RhoA [2]. The Rho kinase inhibitor Y27632 was used to block this Rho effector kinase [12]. A time point of 6 hr was selected because in a previous study in the MC3T3-E1 cells these two inhibitors affected a biological endpoint, caspase-3 activity, at this time point [14]. Figure 2 shows that treatment of MC3T3-E1 cells for 6 hr with either the geranylgeranyl transferase inhibitor GGTI-2166 or the Rho kinase inhibitor Y-27632 elicited dose-dependent loss of actin stress fibers and attenuation of focal adhesions. Figure 2A shows representative confocal micrographs of MC3T3-E1 cells from the control and treatment groups, with images (left to right) of the overlay (F-actin + vinculin), F-actin alone and vinculin alone. Control cells are shown at the top of the figure; effects of two concentrations of the inhibitors, 3 and 30 μM, are seen in images below.

Quantification of the images as described in the Methods showed that actin stress fiber density (Figure 2 B, F), focal adhesion density (Figure 2 D, H), and focal adhesion size (Figure 2 E, I) were decreased dose-dependently by GGTI-2166 and Y-27632. A GGTI concentration of 3 μM elicited significant decreases, and responses were not significantly greater at concentrations of 10 and 30 μM. Y-27632 had significant effects at a concentration of 1 μM, and progressively greater effects were seen over the 1–30 μM concentration range. The tested concentrations of GGTI-2166 and Y-27632 did not lead to statistically significant reductions in edge actin bundle density (Figure 2 C,G), however 1 μM Y-27632 resulted in edge actin bundle density that was greater than control. No treatment resulted in a cellular area or circularity different from control (data not shown).

Based on the finding that inhibiting geranylgeranylation with a geranylgeranyl transferase I inhibitor in the osteoblastic cells led to breakdown of cytoskeletal structures, it was of interest to determine whether a N-containing bisphosphonate, which inhibits the production of

geranylgeranyl groups by inhibiting farnesyl pyrophosphate synthase [3] could also affect the actin cytoskeleton. Although 6 hr treatment with 50 μM alendronate mimicked the effects of GGTI-2166 and Y27632 to cause reduction in actin stress fibers and focal adhesions in some experiments with normal MC3T3-E1 cells (data not shown), effects of longer treatment were more consistent. 22 hr treatment with 50 μM alendronate invariably decreased actin stress fiber density, focal adhesion density and focal adhesion size (Figure 3 A,B,D,E). As was observed with the other inhibitors, edge actin bundle density (Figure 3 C), and cellular area and circularity (data not shown) were not affected. Since effects on focal adhesion density and focal adhesion size paralleled those on the actin stress fibers, only actin stress fibers were quantified in some of the subsequent experiments.

Several agents activating the pathway were tested to determine whether and at which steps they might antagonize the effects of the inhibitors on the cytoskeleton. Co-treatment for 6 hr with the geranylgeranyl group donor GGOH (40 μM) antagonized the effects of the alendronate on actin stress fibers and focal adhesions (Figure 3 A,B,D,E). However, co-treatment with GGOH failed to reverse the reduction in stress fiber density induced by the downstream inhibitors GGTI-2166 (10 μM) and Y-27632 (10 μM) (Figure 4). Transient transfection of MC3T3-E1 cells with a constitutively active RhoA construct (RhoA63L) prevented the inhibitory effects of 6 hr treatment with 50 μM alendronate as well as 6 hr treatment with 10 μM GGTI-2166, but did not prevent the reduction of stress fiber density produced by 6 hr treatment with the Rho kinase inhibitor Y-27632 (10 μM) (Figure 5 A–D).

It was of interest to investigate the effect of PTH on the responses elicited by the inhibitors, since both PTH 1–34 and PTH 3–34, at equivalent concentrations, elicited RhoA translocation in osteoblastic cells [4]. However, it was previously shown that PTH 1–34 promoted transient breakdown of the actin cytoskeleton through a cAMP-dependent pathway [5,6]. PTH 3–34 has little or no stimulatory effects on cAMP, even at concentrations as high as 10^{-7}M [9,15]. In cultures co-treated for 22 hr with alendronate and either PTH 1–34 at 30 nM, or PTH 3–34 at 500 nM, only the PTH 3–34 significantly antagonized the effect of alendronate (Figure 6 A, B). In a second series, a higher concentration of PTH 1–34, 100 nM, was tested and the effects compared with those of the same concentration, 100 nM, of PTH 3–34. Again, co-treatment with PTH 3–34 (100 nM) for 22 hours, but not PTH 1–34 (100 nM), significantly antagonized the effect of alendronate (50 μM) on stress fiber density (Figure 6 C,D). Neither PTH molecule affected edge actin bundle, cellular area or circularity, either alone or in combination with the bisphosphonate.

DISCUSSION

The purpose of the current study was to determine the role of RhoA signaling on the cytoskeleton of osteoblastic cells. The small G proteins are molecular switches that function through binding and hydrolyzing GTP. Their association with GTP is stimulated by guanine nucleotide exchange factors (GEFs) which promote the exchange of GDP for GTP. Small G proteins are found both in the cytoplasm and the plasma membrane, and their translocation as well as their interaction with GEFs are increased by posttranslational lipid modification [16, 17]. The Rho small G proteins, a subfamily of the Ras family, are proteins of molecular weight in the 20–30 kDa range [17–19], and their translocation is promoted by geranylgeranylation at the C-terminus [20]. They act through target proteins, including Rho kinase [21]. Rho small G proteins promote the formation of actin stress fibers and focal adhesions [2], the macromolecular complex through which the cell adheres to the extracellular matrix. These structures are important for cell compaction and shape changes after clustering of cadherin at sites of new cell-cell contacts [22]. Rho is critical for monocyte adhesion and spreading [23] and permeability function of vascular endothelial cells [24]. These cytoskeletal functions are likely to also be relevant for the activities and survival of osteoblasts, which is supported by

the finding that the disruption of focal adhesions in UMR-106.01 cells decreased the expression of the antiapoptotic molecule Bcl-2 and sensitized the cells to TNF-α-induced apoptosis [25].

The findings from the current study are consistent with the model illustrated in Figure 7, which shows the sites and mechanisms of action of the pharmacological agents used in the current study that are based on the literature [3,12,26]. Treatment of MC3T3-E1 osteoblastic cells with the geranylgeranyl transferase I inhibitor GGTI-2166, the Rho kinase inhibitor Y-27632, or the N-containing bisphosphonate alendronate, which through its effects to inhibit farnesyl pyrophosphate synthetase [3] also decreases the availability of geranylgeranyl groups, reduced stress fiber density, focal adhesion density and size, but not edge actin bundle density, cellular area, or circularity. Our results in osteoblastic cells are consistent with previous findings that RhoA is involved in the maintenance of the actin cytoskeleton [2]. The lack of effect on the edge actin bundle is consistent with published findings showing that this structure, which is composed of α-actinin and myosin as well as actin, is more resistant than normal actin stress fibers to treatments that depolymerize F-actin [27]. The lack of effect on the edge actin bundle may also account for the observations that cell circularity was unaffected, the decrease in actin stress fibers being insufficient to result in significant change in overall shape. The current findings reveal that the geranylgeranyl group donor GGOH was able to overcome the effects on the cytoskeletal structures of the bisphosphonate, but not those of the the geranylgeranyl transferase I inhibitor GGTI-2166, or the Rho kinase inhibitor Y-27632. By providing an exogenous source of geranylgeranyl groups, GGOH could antagonize the effect of alendronate, a farnesyl pyrophosphate synthase inhibitor that reduces the intracellular availability of the endogenous geranylgeranyl group donor geranylgeranyl pyrophosphate, but could not overcome the effects of GGTI-2166 and Y-27632 that act further downstream in the pathway. A constitutively active RhoA construct was able to overcome the effects of the bisphosphonate and the geranylgeranyl transferase inhibitor, but the effects of inhibition at the Rho kinase step could not be overcome, which is consistent with Rho kinase being a downstream effector.

PTH 3–34 co-treatment antagonized effects of the bisphosphonate on actin stress fiber density. Although the mechanism of this interaction is not established, our previous study [4] showed that PTH 3–34, as well as PTH 1–34, was able to promote RhoA translocation to the plasma membrane and result in its activation, assessed by an assay utilizing binding to the protein Rhotekin. The mechanism of the PTH-stimulated RhoA activation could be through generation of isoprenyl groups or stimulation of geranylgeranyl transferase, although we are unaware of any published evidence for these effects. An alternative pathway is through Gαl2/Gαl3 signaling. Previous work from our laboratory [28] implicated the Gαl2/Gαl3 heterotrimeric G protein family in PTH action to activate phospholipase D. Activation of other membrane receptors that interact with Gαl2/Gαl3 family heterotrimeric G proteins has been shown to lead to activation of p 115 Rho GEF [29], and Gαl2/Gαl3 stimulates Rho-dependent formation of stress fibers and focal adhesions [30]. Studies from our laboratory showed that dominant negative RhoA prevented effects of Gαl2/Gαl3 on phospholipase D [28]. In contrast to the effects of PTH 3–34, treatment with PTH 1–34 failed to protect the cells against the effects of the bisphosphonate on the cytoskeleton in the current studies. Earlier publications have shown that PTH 1–34 can cause a transient breakdown of the actin cytoskeleton through a cAMP-dependent mechanism [6,7]. PKA inhibits Rho GEF [31], and physiological effects mediated by RhoA in cerebral arteries [32,33] and the trabecular network [32,33] have been found to be antagonized by PKA signaling. The cytoskeletal effects of PTH 1–34 mediated through cAMP and those mediated through PLD activation of RhoA could conceivably counteract each other at the time point studied, resulting in the lack of any significant responses to PTH 1–34. The fact that PTH 3–34 has limited ability to stimulate adenylate cyclase, leaving only the RhoA response, could result in the dissimilar cytoskeletal responses seen with PTH 1–34 and PTH 3–34 in the current studies.

The effects of the N-containing bisphosphonate alendronate to cause loss of actin stress fibers and focal adhesions were elicited with a concentration of 50 μM. In preliminary studies, we found that lower concentrations elicited less dramatic cytoskeletal responses. Cytoskeletal effects of the bisphosphonate were seen at 6 hr, but most consistently at 22 hr. Since bisphosphonates are concentrated in bone, it is difficult to know what *in vitro* concentrations would represent those encountered by bone cells under therapeutic or pathophysiological conditions, especially in states associated with high bone turnover, such as malignancies that have been treated with bisphosphonates. Another recent study has used concentrations of 50 μM and 100 μM alendronate to inhibit protein prenylation in osteoblasts, and found that these concentrations promoted osteoblast apoptosis and inhibited mineralization in 48 hr cultures [34].

It will be important to determine the significance of these structural changes for the biological functions of the osteoblasts and consequently, the importance of the pathway in biological functions. In other studies, we have found that 6 hr treatment with the same concentrations of GGTI-2166, Y27632 [14] and 22 hr treatment with the concentration of alendronate used currently (unpublished) all promote apoptosis of the MC3T3-E1 cells, as indicated by increased caspase3 activity. Although the cell densities used in the assay of caspase activity are different from what are used for the cytoskeletal measurements, the findings could suggest that the cytoskeletal and survival responses are related related. The mechanism of the probable association between survival and cytoskeletal integrity remains to be established, but cell adhesion is likely to play a role [35,36]. In contrast, in preliminary studies, we have not found significant effects of GGTI-2166 treatment on markers of osteoblast differentiation. The role of the pathway in other osteoblast functions, such as cell motility, cell attachment to substrate, cell-cell attachment and the activation of osteoclast precursors are of interest for future investigations.

In summary, we have found that modulation of RhoA has significant effects on the actin cytoskeleton of osteoblastic cells. The current findings could also be relevant to both the function and survival of osteoblasts, and could play a role in the actions of therapeutic pharmacological agents on bone.

ACKNOWLEDGEMENTS

This study was supported by NIH grant AR11262 to PHS. The Medical Student Summer Research Program of Northwestern University's Feinberg School of Medicine provided stipend support for Nikolas H. Kazmers. Dr. Said Sebti, Moffitt Cancer Center and Research Institute and Andrew Hamilton , Yale Unversity kindly donated the GGTI-2166 reagent and Dr Sebti also provided the constitutively active RhoA plasmid; Dr. Alfred Reszka, Merck Research Laboratories, kindly donated the alendronate. We thank Dr. Richard Miller for his generosity in granting us time in his confocal microscopy facility, Dr. Jun Wang for the preparation of the RhoA plasmid for transfection, and for his helpful input, Drs. Tomohiko Yoshida, Zhendong Hong, Dongjun Ren, Philip Hockberger and James Bartles for helpful discussions, and Shirley Foster for her input in the laboratory. Some of the findings in this manuscript were reported at the American Society for Bone and Mineral Research meeting on Targeting Bone Remodeling for the Treatment of Osteoporosis, December 2007.

REFERENCES

1. Diener A, Nebe B, Luthen F, Becker P, Beck U, Neumann HG, Rychly J. Control of focal adhesion dynamics by material surface characteristics. Biomaterials 2005;26:383–392. [PubMed: 15275812]
2. Ridley AJ, Hall A. A The small GTP-binding protein rho regulates the assembly of focal adhesions and actin stress fibers in response to growth factors. Cell 1992;70:389–399. [PubMed: 1643657]
3. Bergstrom JD, Bostedor RG, Masarachia PJ, Reszka AA, Rodan G. Alendronate is aspecific nanomolar inhibitor of farnesyl diphosphate synthase. Arch Biochem Biophys 2000;373:231–241. [PubMed: 10620343]

4. Radeff JM, Nagy Z, SternPH Rho Rho. Rho kinase are involved in parathyroid hormone-stimulated protein kinase C alpha translocation and IL-6 promoter activity in osteoblastic cells. J Bone Miner Res 2004;19:1882–1891. [PubMed: 15476589]
5. Lomri A, Marie PJ. Distinct effects of calcium-and cyclic AMP-enhancing factors on cytoskeletal synthesis and assembly in mouse osteoblastic cells. Biochim Biophys Acta 1990;1052:179–186. [PubMed: 1691023]
6. Egan JJ, Gronowicz G, Rodan GA. Parathyroid hormone promotes the disassembly of cytoskeletal actin and myosin in cultured osteoblastic cells: mediation by cyclic AMP. J Cell Biochem 1991;45:101–111. [PubMed: 1848561]
7. Lomri A, Marie PJ. Changes in cytoskeletal proteins in response to parathyroid hormone and 1,25-dihydroxyvitamin D in human osteoblastic cells. Bone Miner 1990;10:1–12. [PubMed: 2168775]
8. Zhang J, Ryder KD, Bethel JA, Ramirez R, Duncan RL. PTH-induced actin depolymerization increases mechanosensitive channel activity to enhance mechanically stimulated Ca2 + signaling in osteoblasts. J Bone Miner Res 2006;21:1729–1737. [PubMed: 17002579]
9. Donahue HJ, Fryer MJ, Eriksen EF, Heath H 3rd. Differential effects of parathyroid hormone and its analogues on cytosolic calcium ion and cAMP levels in cultured rat osteoblast-like cells. J Biol Chem 1988;263:13522–13527. [PubMed: 2843523]
10. Fujimori A, Cheng SL, Avioli LV, Civitelli R. Structure-function relationship of parathyroid hormone: activation of phospholipase-C, protein kinase-A and -C in osteosarcoma cells. Endocrinology 1992;130:29–36. [PubMed: 1727705]
11. Sun J, Blaskovich MA, Knowles D, Qian Y, Ohkanda J, Bailey RD, Hamilton AD, Sebti SM. Antitumor efficacy of a novel class of non-thiol-containing peptidomimetic inhibitors of farnesyltransferase and geranylgeranyltransferase I: combination therapy with the cytotoxic agents cisplatin, Taxol, and gemcitabine. Cancer Res 1999;59:4919–4926. [PubMed: 10519405]
12. Ishizaki T, Uehata M, Tamechika I, Keel J, Nonomma K, Maekawa M, Naruyima S. Pharmacological properties of Y-27632, a specific inhibitor of Rho-associated kinase. Mol Pharmacol 2000;57:976–983. [PubMed: 10779382]
13. Gonon EM, Skalski M, Kean M, Coppolino MG. SNARE-mediated membrane traffic modulates RhoA-regulated focal adhesion formation. FEBS Lett 2005;579:6169–6178. [PubMed: 16243314]
14. Yoshida T, Clark MF, Stern PH. The small GTPase RhoA is crucial for MC3T3-E1 osteoblastic cell survival. J Cell Biochem. 2009in press.
15. Fujimori A, Cheng S-L, Avioli L, Civitelli R. Dissociation of second messenger activation by parathyroid hormone fragments in osteosarcoma cells. Endocrinology 1991;128:3032–3039. [PubMed: 1645259]
16. Zhang F, Casey P. Protein prenylation: molecular mechanisms and functional consequences. Annu Rev Biochem 1996;65:241–269. [PubMed: 8811180]
17. Cohen LH, Pieterman E, van Leeuwen RE, Overhand M, Burm BE, van der Marel GA, van Boom JH. Inhibitors of prenylation of Ras and other G-proteins and their application as therapeutics. Biochem Pharmacol 2000;60:1061–1068. [PubMed: 11007942]
18. Van Aelst L, D'Souza-Schorey C. Rho GTPases and signaling networks. Genes Dev 1997;11:2295–2322. [PubMed: 9308960]
19. Etienne-Manneville, SaH A. Rho GTPases in cell biology. Nature 2002;420:629–635. [PubMed: 12478284]
20. Michaelson D, Silletti J, Murphy G, D'Eustachio P, Rush M, Philips MR. Differential localization of Rho GTPases in live cells: regulation by hypervariable regions RhoGDI binding. J Cell Biol 2001;152:111–126. [PubMed: 11149925]
21. Sakurada S, Okamoto H, Takuwa N, Sugimoto N, Takuwa Y. Rho activation in excitatory agonist-stimulated vascular smooth muscle. Am J Physiol Cell Physiol 2001;281:C571–C578. [PubMed: 11443056]
22. Braga VM. Cell-cell adhesion and signalling. Curr Opin Cell Biol 2002;14:546–556. [PubMed: 12231348]
23. Wojciak-Stothard B, Williams L, Ridley AJ. Monocyte adhesion and spreading on human endothelial cells is dependent on Rho-regulated receptor clustering. J Cell Biol 1999;145:1293–1307. [PubMed: 10366600]

24. van Nieuw Amerongen GP, van Delft S, Vermeer MA, Collard JG, van Hinsbergh VW. Activation of RhoA by thrombin in endothelial hyperpermeability: role of Rho kinase protein tyrosine kinases. Circ Res 2000;87:335–340. [PubMed: 10948069]

25. Triplett JW, Pavalko FM. Disruption of alpha-actinin-integrin interactions at focal adhesions renders osteoblasts susceptible to apoptosis. Am J Physiol Cell Physiol 2006;291:C909–C921. [PubMed: 16807302]

26. Sun J, O J, Coppola D, Yin H, Kothare M, Busciglio B. Geranylgeranyltransferase I inhibitor GGTI-2154 induces breast carcinoma apoptosis and tumor regression in H-Ras transgenic mice. Cancer Res 2003;63:8922–8929. [PubMed: 14695209]

27. Zand MS, Albrecht-Buehler G. What structures, besides adhesions, prevent spread cells from rounding up? Cell Motil Cytoskeleton 1989;13:195–211. [PubMed: 2505936]

28. Singh AT, Gilchrist A, Voyno-Yasenetskaya T, Radeff-Huang JM, Stern PHG. alpha l2/G alpha l3 subunits of heterotrimeric G proteins mediate parathyroid hormone activation of phospholipase D in UMR-106 osteoblastic cells. Endocrinology 2005;146:2171–2175. [PubMed: 15705779]

29. Kozasa T, Jiang X, Hart MJ, Sternweis PM, Singer WD, Gilman AG, Bollag G, Sternweis PC. p115 RhoGEF, a GTPase activating protein for Galpha l2 and Galpha l3. Science 1998;280:2109–2111. [PubMed: 9641915]

30. Buhl AM, Johnson NL, Dhanasekaran N, Johnson GL. G alpha 12, G alpha 13 stimulate Rho-dependent stress fiber formation and focal adhesion assembly. J Biol Chem 1995;270:24631–24634. [PubMed: 7559569]

31. Diviani D, Abuin L, Cotecchia S, Pansier L. Anchoring of both PKA and 14-3-3 inhibits the Rho-GEF activity of the AKAP-Lbc signaling complex. Embo J 2004;23:2811–2820. [PubMed: 15229649]

32. Luykenaar KD, Welsh DG. Activators of the PKA and PKG pathways attenuate RhoA-mediated suppression of the KDR current in cerebral arteries. Am J Physiol Heart Circ Physiol 2007;292:H2654–H2663. [PubMed: 17277021]

33. Shen X, Koga T, Park BC, SundarRaj N, Yue BY. Rho GTPase and cAMP/protein kinase A signaling mediates myocilin-induced alterations in cultured human trabecular meshwork cells. J Biol Chem 2008;283:603–612. [PubMed: 17984096]

34. Idris AI, Rojas J, Greig IR, Van't Hof RJ, Ralston SH. Aminobisphosphonates cause osteoblast apoptosis and inhibit bone nodule formation in vitro. Calcif Tissue Int 2008;82:191–201. [PubMed: 18259679]

35. Wozniak MA, Modzelewska K, Kwong L, Keely PJ. Focal adhesion regulation of cell behavior. Biochim Biophys Acta 2004;1692:103–119. [PubMed: 15246682]

36. Reddig PJ, Juliano RL. Clinging to life: cell to matrix adhesion and cell survival. Cancer Metastasis Rev 2005;24:425–439. [PubMed: 16258730]

Abbreviations

CA RhoA, Constitutively active RhoA; FPP, Farnesyl pyrophosphate; FPP Synthase, Farnesyl pyrophosphate synthase; GG, Geranylgeranyl group; GGOH, Geranylgeraniol; GGPP, Geranylgeranyl pyrophosphate; GGTase I, Geranylgeranyl transferase I; GGTI-2166, Geranylgeranyl transferase I inhibitor; Rho-GEF, Rho guanine nucleotide exchange factor; Y-27632, Rho kinase inhibitor.

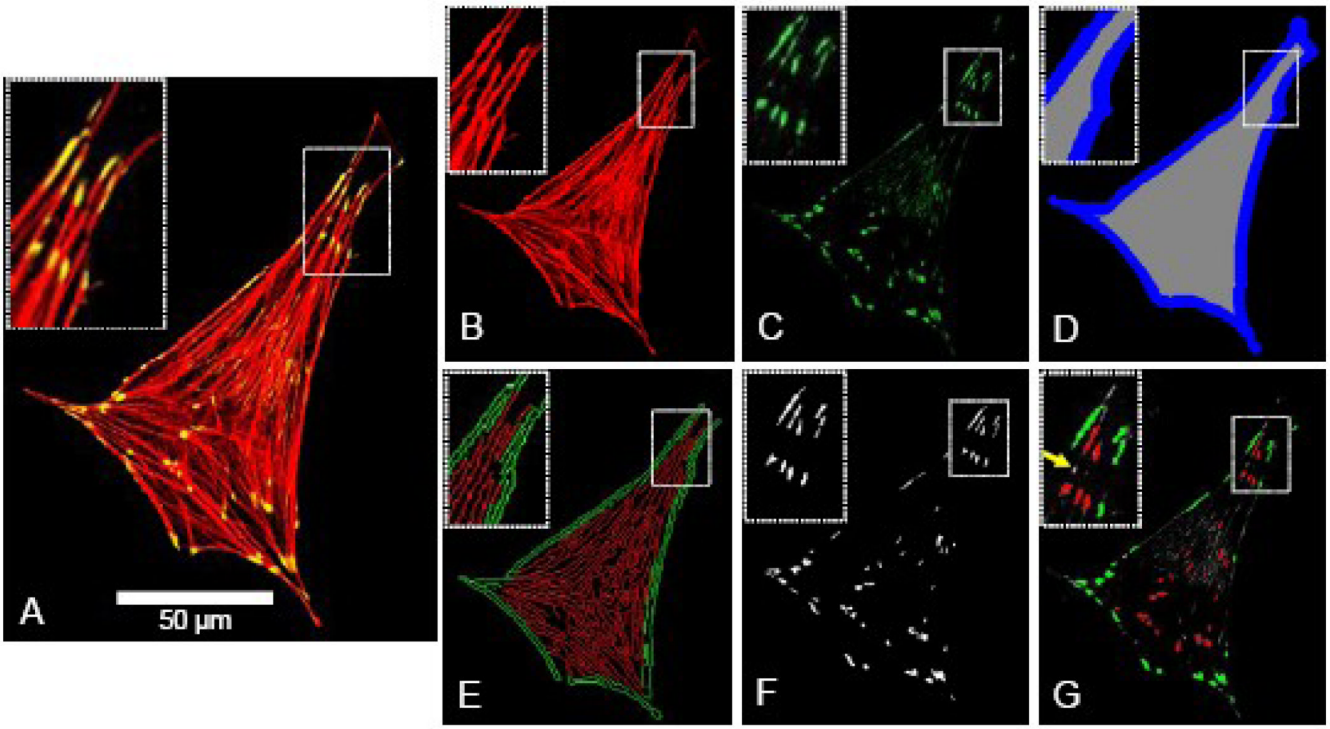

Figure 1.

Images and approach used for image quantification of actin stress fiber density, edge actin bundle density, density and area of focal adhesions, cellular area and circularity, as described in further detail under *Image Quantification* in the Methods. For each cell under examination, the input into the program included three separate images extracted from the original confocal micrograph, including an image of the F-actin + vinculin overlap (Figure 1A), F-actin alone (Figure 1B), and vinculin alone (Figure 1C). The F-actin image was converted to binary, and the cellular area, perimeter, and circularity were calculated. The internal (Figure 1D - gray region) and perimeter (blue region) regions of the cell were defined, corresponding with the locations of the actin stress fibers and actin edge bundle, respectively. The F-actin image (Figure 1B) was normalized for average pixel intensity, intensity-thresholded to minimize background fluorescence, converted to binary, and extraneous objects with an area of ≤0.5 μm^2 were removed. The resulting image was subjected to a Canny filter edge-detecting algorithm, producing an image (Figure 1E) depicting the edges of F-actin fibers in the perimeter (green – edge actin bundle) and internal regions of the cell (red – stress fibers). This image was thresholded by aspect ratio of each detected edge to remove circular non-filamentous artifacts. The area occupied by F-actin edge was computed separately in both the perimeter and internal regions of the cell, and stress fiber density and edge actin bundle density were calculated by normalizing the area occupied by F-actin edge in the internal and perimeter regions of the cell (Figure 1E) by the area of the internal and perimeter regions, respectively. To quantify the focal adhesion density and average size, the vinculin image (Figure 1C) was intensity-thresholded to reduce background fluorescence, converted to binary, and extraneous objects ≤0.3 μm^2 [13] were removed (Figure 1F). Focal adhesion density (focal adhesions per cellular area) and average focal adhesion size were calculated for the cell as a whole. Figure 1G depicts the focal adhesions that were detected based on these criteria (red = internal focal adhesion; green = perimeter focal adhesion; yellow arrow = vinculin aggregate below area threshold of 0.3 μm^2).

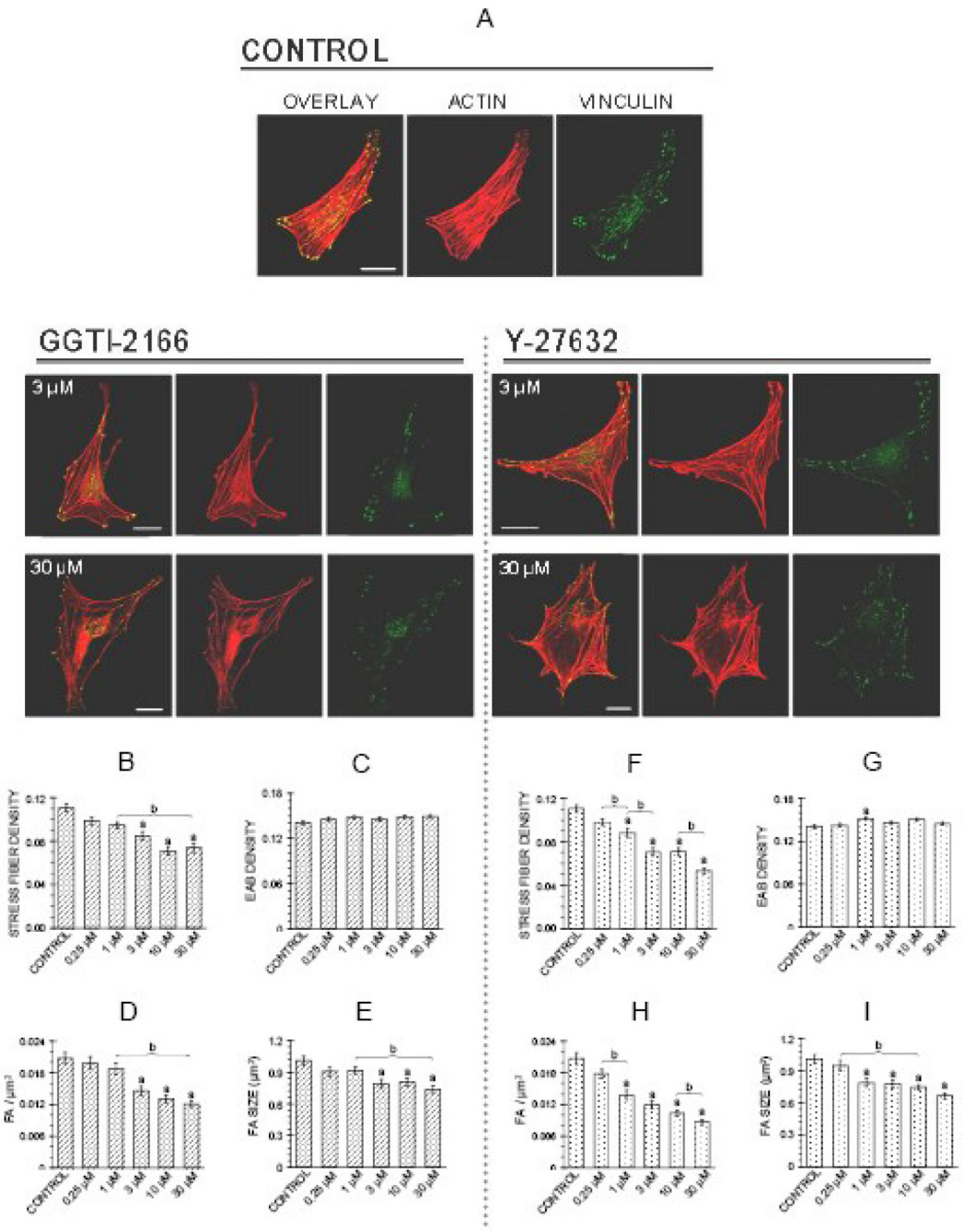

Figure 2.

Geranylgeranyl transferase I inhibitor GGTI-2166 (left panel) or Rho kinase inhibitor Y-27632 (right panel) decrease stress fiber density, focal adhesion density and focal adhesion area in MC3T3-E1 cells. Treatments were for 6 hr in BSA medium. A: Representative confocal micrographs of cells showing actin stress fibers and focal adhesions. Bars represent 25 μm. B–I: Quantification of parameters. Values are means +/− SEM of responses measured in 3 independent experiments in which 40 cells were imaged and quantified per group. There are no statistically significant differences in edge actin bundle (2C, 2G), cellular area, or circularity (data not shown). Different letters indicate statistically significant differences (95% Tukey confidence interval) from control (a) and between groups (b).

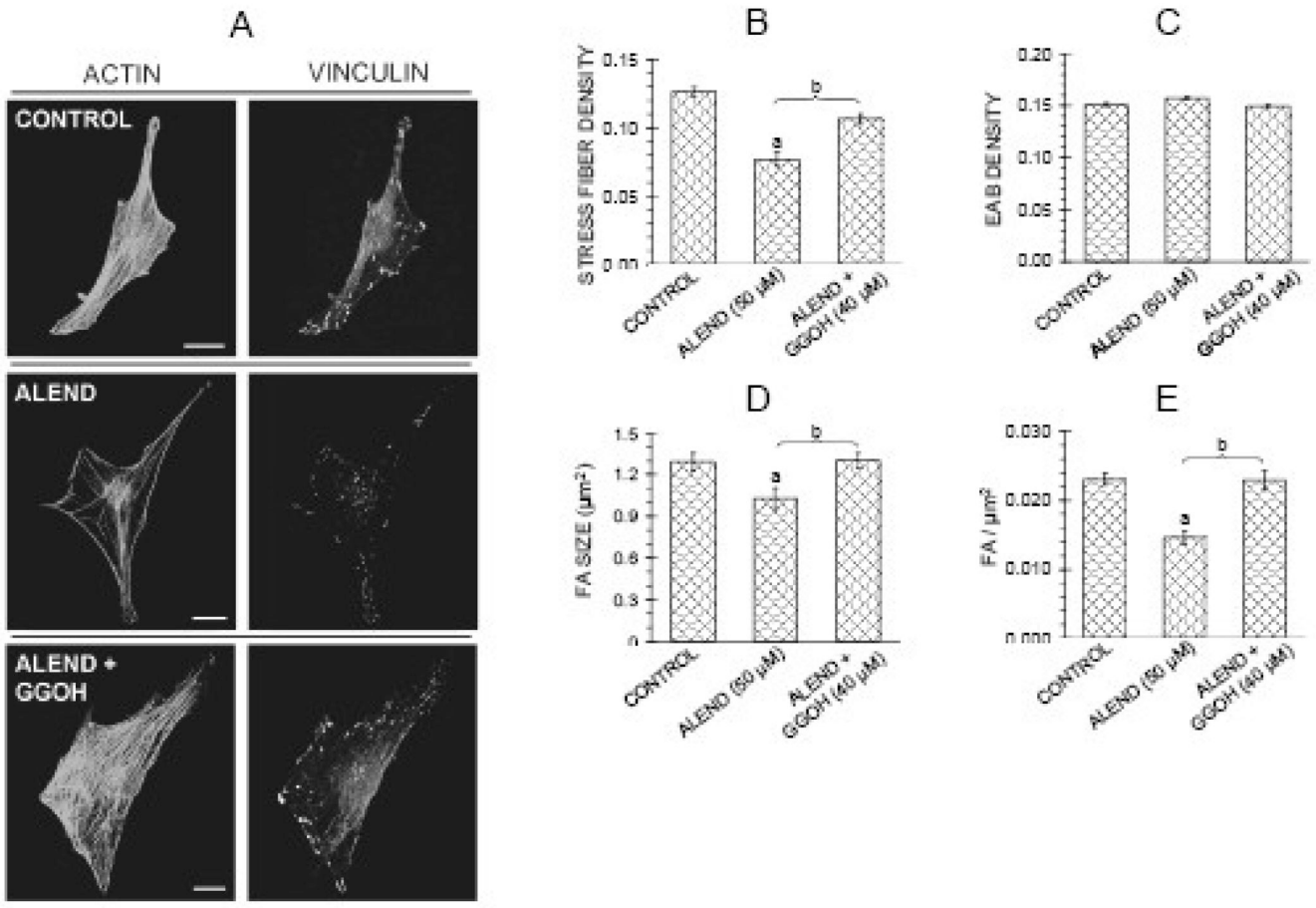

Figure 3.

Alendronate (50 μM) decreases stress fiber density, focal adhesion density, and focal adhesion area in MC3T3-E1 cells, and effects are antagonized by geranylgeranyl group donor geranylgeraniol (GGOH) (40 μM). Treatments were for 22 hr in FBS medium. A: Confocal micrographs of cells showing actin stress fibers and focal adhesions. Bars represent 25 μm. B–E: Quantification of parameters. Values are means +/− SEM of responses measured in 2 independent experiments in which 40 cells were imaged and quantified per group. Different letters indicate statistically significant differences (95% Tukey confidence interval) from control (a) and between groups (b). There are no statistically significant differences in edge actin bundle (3C), cellular area or circularity (data not shown).

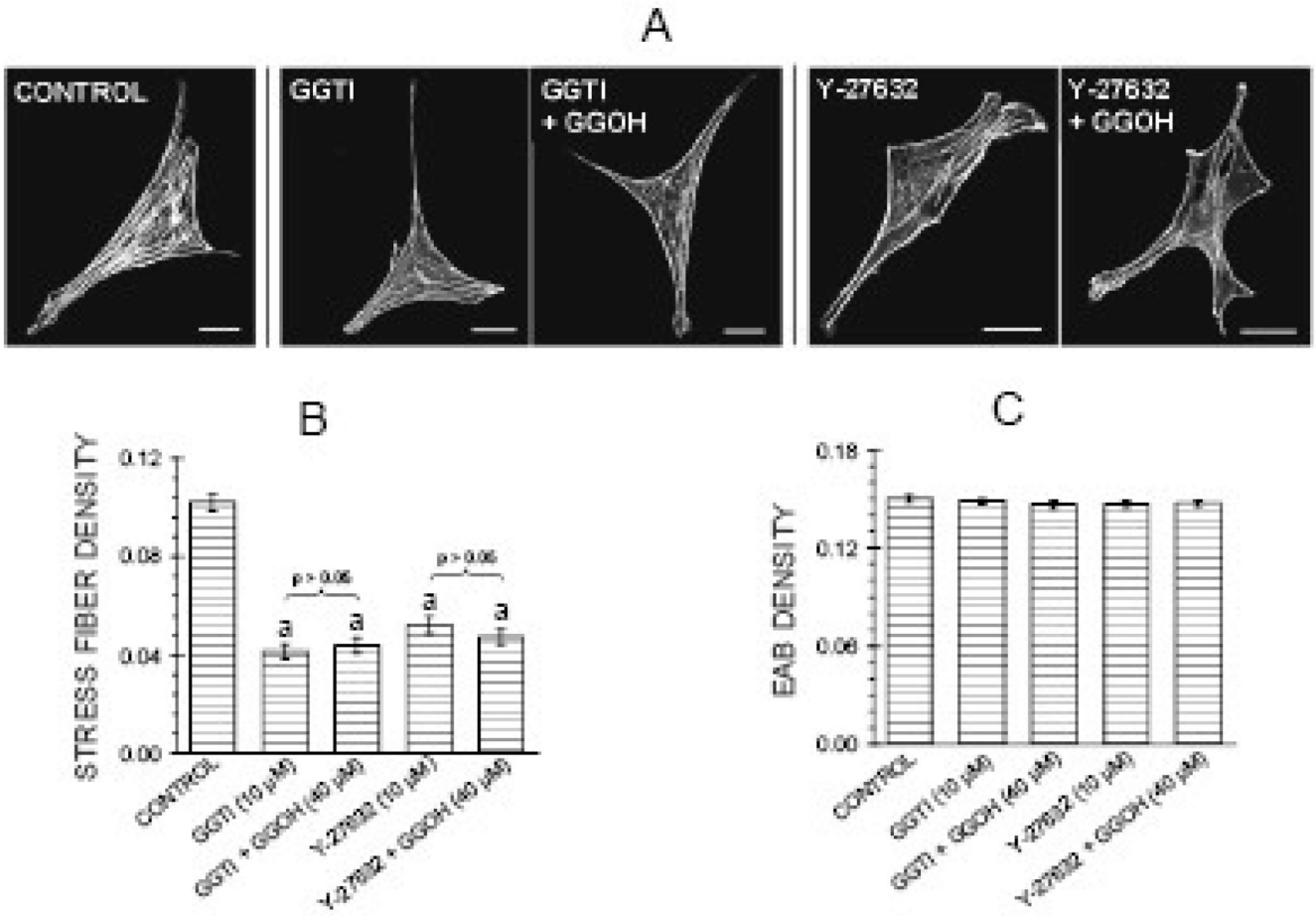

Figure 4.

Geranylgeranyl group donor geranylgeraniol (GGOH) (40 μM) fails to antagonize effects of GGTI-2166 (10 μM) or Y-27632 (10 μM) on actin stress fibers. Treatments were for 6 hr in BSA medium. A: Confocal micrographs of cells showing actin stress fibers and focal adhesions. Bars represent 25 μm. B, C: Quantification of parameters. Values are means +/−SEM of responses measured in 2 independent experiments in which 40 cells were imaged and quantified per group. There are no statistically significant differences in edge actin bundle (4C), cellular area, or circularity (data not shown)

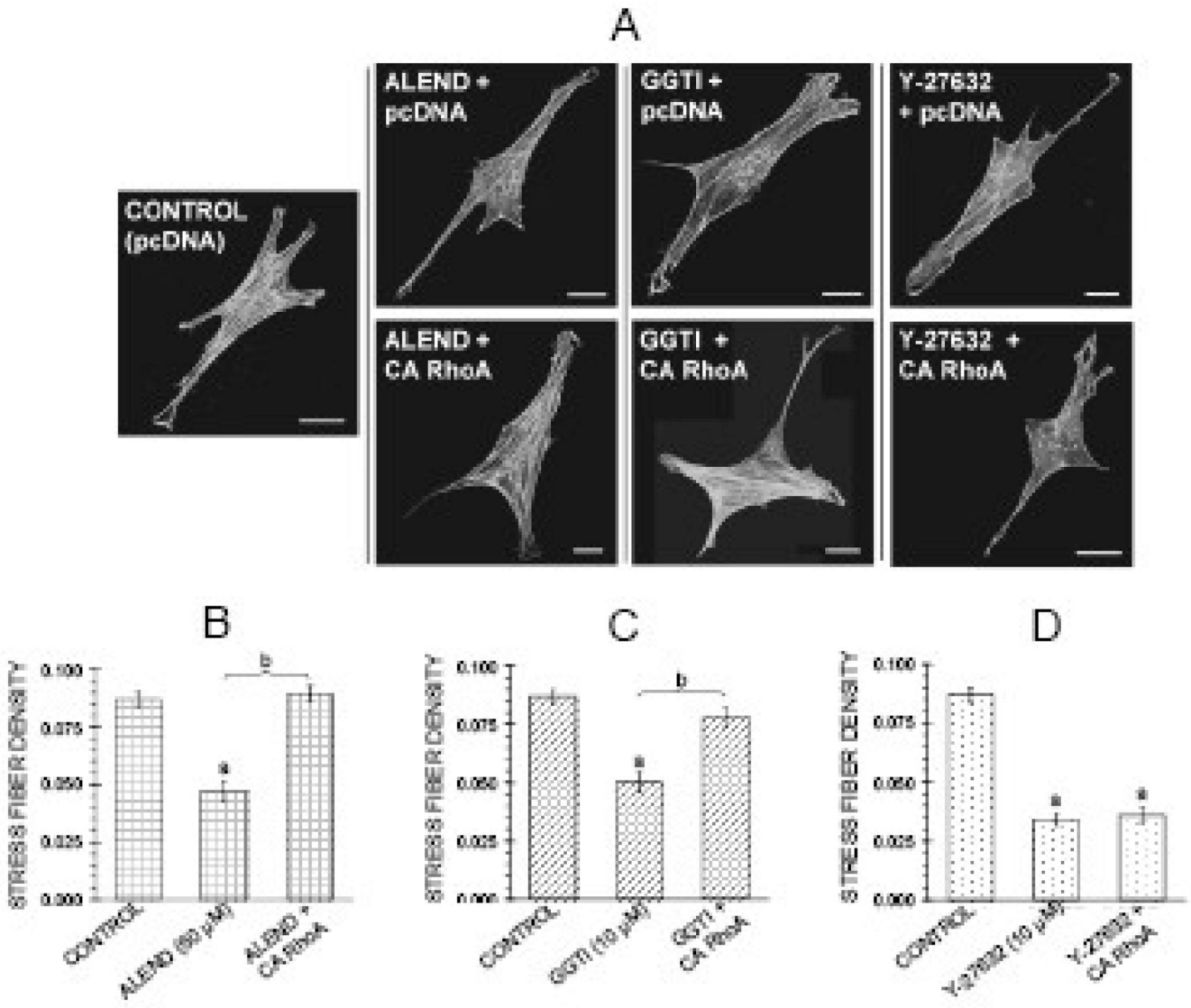

Figure 5.

Constitutively active RhoA antagonizes effect of alendronate (50 μM) and GGTI-2166 (10 μM), but not Y-27632 (10 μM) on actin stress fibers in MC3T3-E1 cells. After transfection, cells were treated for 6 hr with alendronate, GGTI-2166, or and Y-27632 in BSA media. A: Confocal micrographs of cells showing actin stress fibers. Bars represent 25 μm. B–D: Quantification of parameters. Values are means +/− SEM of responses measured in 2 independent experiments in which 40 cells were imaged and quantified per group. Different letters indicate statistically significant differences (95% Tukey confidence interval) from control (a) and between groups (b). There are no statistically significant differences in edge actin bundle, cellular area, or circularity (data not shown).

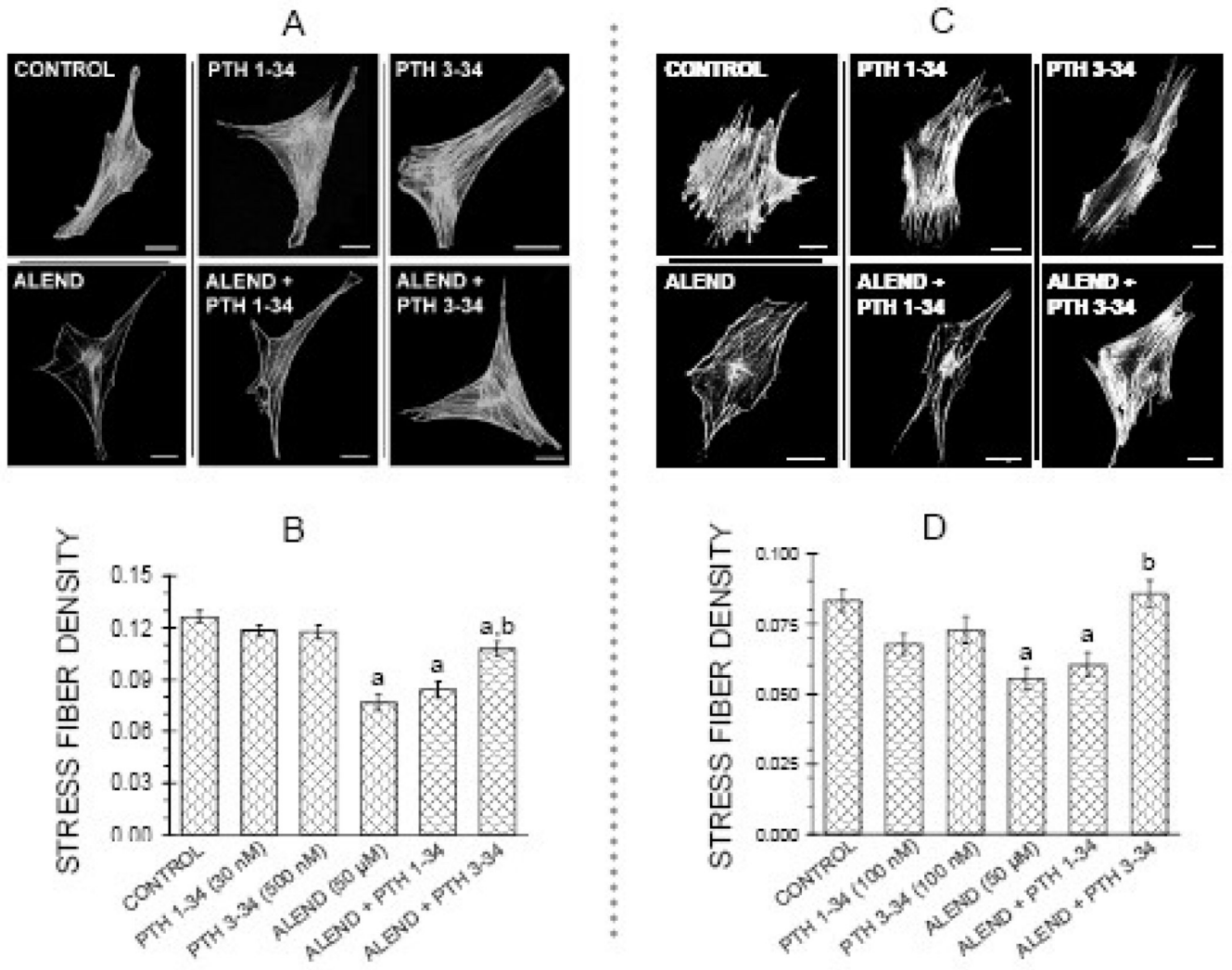

Figure 6.

PTH 3–34, antagonizes effect of alendronate (50 μM) on actin stress fibers in MC3T3-El cells, but PTH 1–34 does not. Treatments were for 22 hr in FBS media. A: Confocal micrographs of cells showing actin stress fibers. Bars represent 25 μm.; B: Quantification of parameters with treatment with 30 nM PTH 1–34 or 500 nM 3–34. C: Quantification of parameters with treatment with 100 nM PTH 1–34 or 100 nM PTH 3–34. Values are means +/−SEM of responses measured in 2 independent experiments in which 30–40 cells were imaged and quantified per group. Different letters indicate statistically significant differences (95% Tukey confidence interval) from control (a) and between groups (b). There are no statistically significant differences in edge actin bundle, cellular area, or circularity (data not shown).

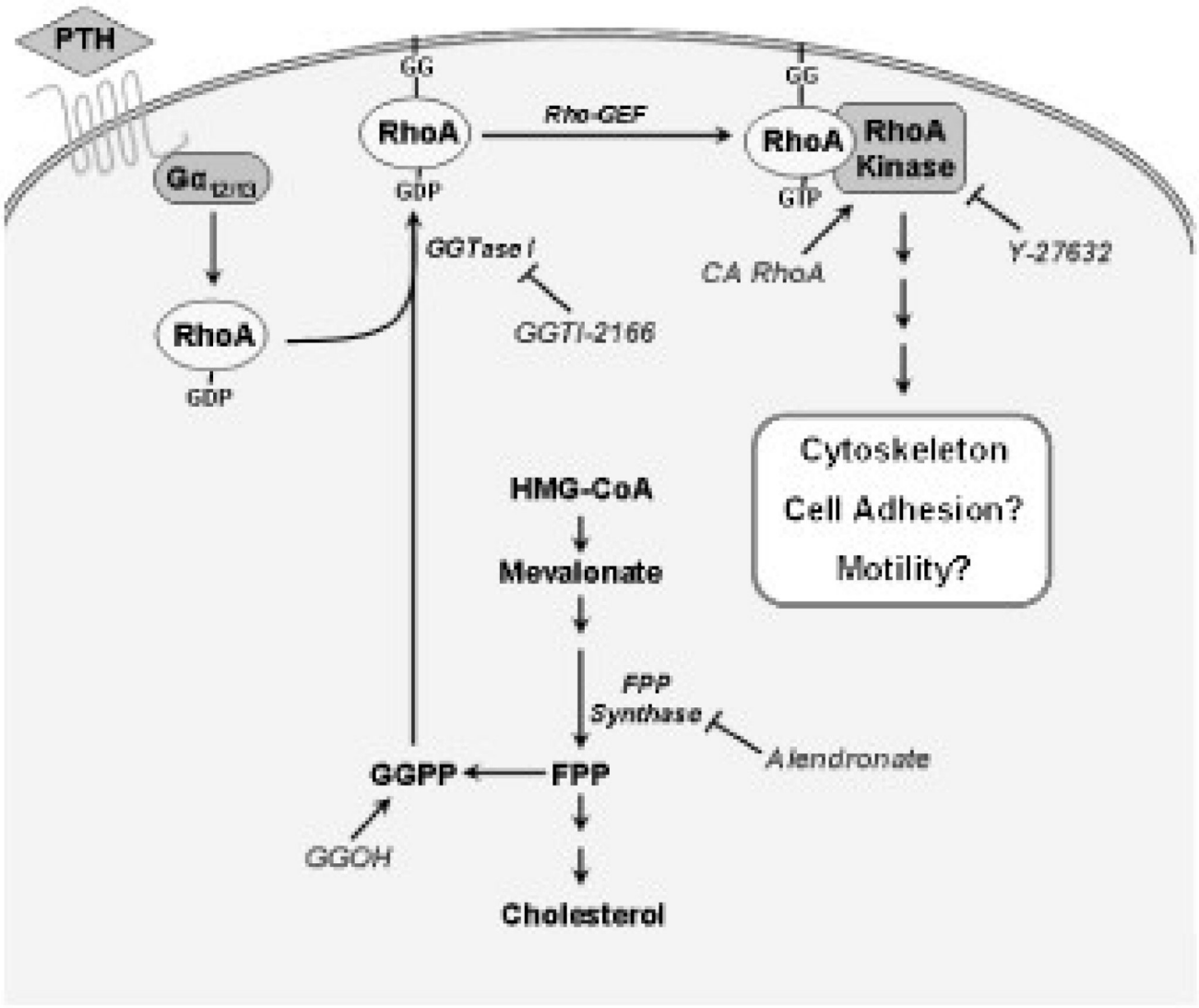

Figure 7.
Proposed pathway involved in the regulation of the osteoblast F-actin cytoskeleton, based upon previous literature and the current experimental results.